Mesh Independence Study on CFD for Cryo-CO_2 Cooling Strategy

Nur Fatini Mohamad Fauzee, Nurul Hayati Abdul Halim[*]*, Zainoor Hailmee Solihin, Izdihar Tharazi, Nor Hayati Saad, Zulaika Zulkifli*
School of Mechanical Engineering, College of Engineering,
Universiti Teknologi MARA, 40450, Shah Alam, Selangor, MALAYSIA
[*]*hayatihalim@uitm.edu.my*

Musfirah Abdul Hadi
Faculty of Manufacturing and Mechatronic Engineering,
Universiti Malaysia Pahang, 26600, Pekan, Pahang, MALAYSIA

ABSTRACT

This study conducts comprehensive mesh independence tests to identify the optimum mesh independence parameters that offer the most feasible Computational Fluid Dynamic (CFD) analysis on cryo-CO_2 temperature variations and its heat transfer performance under cryo-CO_2 cooling strategy in metal cutting. ANSYS Fluent was used to conduct the CFD study with its mesh control parameters (relevance center and smoothing) designed using Response Surface Methodology (RSM) under Central Composite Design (CCD). An Analysis of Variance (ANOVA) was applied to analyse how the controlled factors influenced the cryo-CO_2 flow temperature when it flowed from the nozzle to the tooltip. The analysis found that the relevance centre was more significant in influencing the accuracy of the response value. For optimization, the combination of medium relevance center and smoothing meshes was suggested to develop the lowest cryo-CO_2 flow temperature at 256.85 K. This is crucial since most machining outputs are heat dependent. Experimental data sets were used to validate the predicted result. Distances between 3.6 to 18 mm showed an acceptable deviation of ~0.4 – 0.6% and ~0.4 – 4.2% for simulated and experimented work, respectively. This value is acceptable, and the generated quadratic model equation can be applied for prediction. The heat transfer performance of the cryo-CO_2 flow at tool-chip and tool-workpiece interfaces under high-speed machining was also discussed. Moreover, further analysis using the optimal solution has led to a better understanding of heat transfer in cryogenic carbon dioxide (CO_2), resulting in enhanced cooling of the cutting zone and improved machining processes.

ISSN 1823-5514, eISSN 2550-164X
Received for review: 2023-11-01
Accepted for publication: 2023-12-20
Published: 2024-01-15

https://doi.org/10.24191/jmeche.v21i1.25372

Keywords: *Mesh Independence; Cryogenic; CFD Simulation; Heat Transfer; Analysis of Variance (ANOVA); Response Surface Methodology (RSM)*

Introduction

In recent years, researchers have become increasingly interested in using cryogenic carbon dioxide (Cryo-CO_2) as a coolant during metal-cutting processes. Cryo-CO_2, which has a temperature of -76 ℃, is considered an alternative to liquid nitrogen (-196 ℃) for cooling purposes. This shift towards cryo-CO_2 is driven by its effectiveness in reducing cutting temperatures and minimizing potential negative effects on both workpieces and cutting tools, such as work-hardening and thermal shock [1]–[3]. The intermittent cutting process in high-speed milling subjects the tool to significant temperature fluctuations. These rapid changes can lead to fatigue and the formation of cracks due to constant contraction and expansion. Cryo-CO_2 has shown promising results as a coolant in high-speed milling, particularly for difficult-to-machine where researchers such as Halim et al. [4] found that utilizing cryo-CO_2 instead of liquid nitrogen (LN_2) can lead to improvements in tool life and surface finish. This aligns with similar studies conducted by Pereira et al. [5] and Dilip and Pradeep [6], which also highlight the advantages of using CO_2 instead of LN_2 for high-speed cutting operations. Thus, understanding the behaviour of cryogenic flows and optimizing flow systems for different applications is essential for achieving optimal metal-cutting performance.

However, accurately investigating the complex flow characteristics and properties of cryogenic coolant by experimental work poses technological challenges, as highlighted by Tahmasebi et al. [7]. Other researchers, such as Jamil et al. [8] and Kumar et al. [9], also found that complex flow patterns, heat transfer mechanisms, and temperature distributions were not easily observable through experiments alone. However, there are limitations to consider, such as the need for specialized equipment and infrastructure to handle and store extremely cold gas, which can pose challenges in continuous supply and management. Hence, regular monitoring and maintenance are necessary to ensure efficient utilization of cryo-CO_2.

Therefore, it is crucial to comprehend the properties and dynamics of cryo-CO_2 through Computational Fluid Dynamics (CFD) simulations. The accuracy of CFD analysis is essential for understanding the flow characteristics and temperature distribution of CO_2, as it relies on mathematical models that approximate fluid behaviour. This approach provides a suitable alternative to experimental studies, particularly when investigating how cryo-CO_2 flow affects high-speed cutting in the cutting zone. Research conducted by Pereira et al. [5], Gamidi et al. [10], and Salame et al. [13] supported these claims as they applied the CFD to their studies of coolant flow. Moreover, researchers increasingly use CFD for its visual

representations of flow fields in simulations, time-saving efficiency, and accuracy for predicting the performance of real-world products [11]. Through these simulation-based approaches, both researchers gained valuable insights into the impact of various cooling technologies on machining processes. DEFORM software analysis was employed to examine the coolant behaviour and temperature distribution in titanium alloy drilling, in contrast to Mohan et al. [12]. Although utilising different software, simulative work was preferred over experimental approaches due to its enhanced efficiency in providing detailed insights and scalability for optimizing cooling systems and reducing cutting temperatures at the cutting zone.

In this context, combining mesh independence in the study of cryo-CO_2 flow behaviour is essential by modifying different parameters and comparing their corresponding results to ensure accurate predictions. This analysis allows for determining an optimal level of refinement that guarantees enhanced coolant penetration into the cutting zone, resulting in improved heat dissipation and preventing excessive temperature rise. Ultimately, this approach minimizes workpiece thermal damage and improves machining efficiency. By this, Sadrehaghighi [13], Gamidi et al. [10], and Hendry et al. [14] have demonstrated the significance of conducting mesh independence studies in CFD simulations to determine the optimal stage at which further refinement of the mesh is no longer necessary as achieving an appropriate level of mesh resolution is crucial for ensuring the accuracy and reliability of this approach. In order to assess the impact on the converged solution, researchers often conduct CFD together with mesh independence studies with different levels of mesh resolutions [9], [14]-[15]. Alternative approaches, such as conducting a mesh sensitivity analysis, have been reported by past researchers such as Caudill et al. [16] and Hamza Abdul Sada [17]. These studies have shown that performing simulations with different levels of mesh density aids in evaluating the convergence and reliability of the results.

Thus, the primary aim of this study is to perform a mesh independence analysis of cryo-CO_2 in high-speed cutting. The purpose is to determine an appropriate and trustworthy mesh that can provide the desired level of accuracy for modelling the heat transfer flow characteristics during the machining process using cryo-CO_2. It is crucial to accurately represent the physical phenomena involved to achieve reliable simulation results.

Mathematical Modelling

Governing equations

By applying the conservation of energy principle [18], the total energy and the energy generated in a system are equal to the sum of changes in internal energy and the energy output. According to the first law of thermodynamics, this can be expressed as in Equation (1):

$$E_{in} + E_{gen} = \Delta U + E_{out} \quad (1)$$

By referring to Figure 1, the sum of the energy transferred by conduction and net energy generation within the control volume equals the change in internal energy within the control volume.

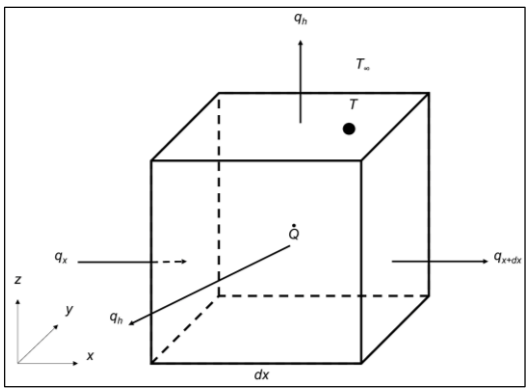

Figure 1: Control volume in Cartesian coordinates

Therefore, the energy balance in the *x*-direction can be expressed as shown in Equation (2).

$$q_x\, dt + \dot{Q}\, dx\, dt = \Delta U + q_{x+dx}\ dt + q_h\, dx\, dt \quad (2)$$

where q_x represents the heat transfer from the cutting zone of the x-direction, and $\dot{Q}$ (in kW/m^2) is the heat generated from the milling process's heat source. Equation (2) can be rearranged into Equation (3).

$$q_x\, dt - q_{x+dx}\ dt - q_h P\, dx\, dt + \dot{Q}\, dx\, dt = \Delta U \quad (3)$$

Within the control volume, heat is conducted through the material from one side to another. According to Fourier's law, the heat conducted into the system, q_x or heat flux (in kW/m^3), describes the thermal conductivity, while K (in kW/m.°C) of the material determines how well it conducts heat. The cross-sectional area (A) and the temperature gradient $\left(\frac{dT}{dx}\right)$ play a role in quantifying the heat being conducted.

The influence of heat conduction in the *x*-direction on the comprehensive heat transfer model was determined by a $K_x.dx.dy.dz\frac{\partial^2 T}{dx^2}$. Here, K_x represents the thermal conductivity in the x-direction, which varies based on the coordinates *x*, *y*, and *z*. When multiplied by $dx.dy.dz$, and *t*, these

factor yields the volume element in the *x*-, *y*-, and *z*-directions, respectively, as this model was aimed to depict three-dimensional cryo-CO_2 flow.

According to the heat transfer analogy, the equation for heat conduction in a solid can be linked to the equation for convection from the cryogenic coolant to the cutting zone by considering how the heat flux is related to the temperature difference between fluid and solid surface. This relationship was described by an overall heat transfer coefficient, which takes into account both conduction and convection processes. In line with Lequien et al. [19], the equation for convection from the cryogenic coolant to the cutting zone can be calculated from the expressions of $q_h = hA\ (\Delta T)$. When q_h (in kW/m^2), it was denoted as the heat flux. A (in m^2) represented for the constant parameter of the solid's convective surface area in contact with the fluid, and ΔT signified the temperature difference between T_w, which is the hot surface temperature at the workpiece, and T_∞ represented the fluid bulk. Here, $\Delta T = T_w - T_\infty$. The variable T_w was denoted the temperature of solid surface exposed to the fluid, while T_∞ refered to the fluid temperature.

Thus, the general Equation (4) for three-dimensional heat conduction combined with convection is expressed by:

$$\left[K\left(\frac{\partial^2 T}{dx^2}+\frac{\partial^2 T}{dy^2}+\frac{\partial^2 T}{dz^2}\right)\right]-hA\ (\Delta T)+\dot{Q}=\rho c\frac{\partial T}{\partial t} \tag{4}$$

As the heat transfer equation combined, thus it was linked to the cryo-CO_2 model as illustrated in Figure 2. The 2-dimensional model was illustrated before in SpaceClaim in order to generate the 3-dimensional model that was simulated using the commercial CFD approach in ANSYS R1 2023 [20]-[21].

From Equation (4), any differentiation with respect to time is equal to zero because the model in the present study was in a steady-state situation. By referring to the solid and fluid domain of cryo-CO_2 as in Figure 2, the energy conservation can be expressed as:

$$\left[K_w\left(\frac{\partial^2 T_w}{dx^2}+\frac{\partial^2 T_w}{dy^2}+\frac{\partial^2 T_w}{dz^2}\right)\right]+\left[K_t\left(\frac{\partial^2 T_t}{dx^2}+\frac{\partial^2 T_t}{dy^2}+\frac{\partial^2 T_t}{dz^2}\right)\right]-hA\ (\Delta T)_f+\dot{Q}=0 \tag{5}$$

where subscript *w*, *t* and *f* denoted as workpiece, cutting tool and fluid, respectively. Then, the heat transfer coefficient at the dispersed-continuous of cryo-CO_2, which explained the heat transfer, indicated the exchange of thermal energy between two mediums caused by a variation in temperature can be defined as in Equation (6):

$$h=\frac{NuK_f}{L} \tag{6}$$

where, L is the length (mm) of the dispersed-continuous from the nozzle to the tip of cutting tool; K_f is the thermal conductivity of dispersed-continuous of cryo-CO_2, and h is the heat transfer coefficient (in W/m^{2}K) of cryo-CO_2. Meanwhile, the Nusselt number, which is closely linked to Equation (6), as expressed:

$$Nu = 0.102\mathrm{Re}^{0.675}\mathrm{Pr}^{1/3} \tag{7}$$

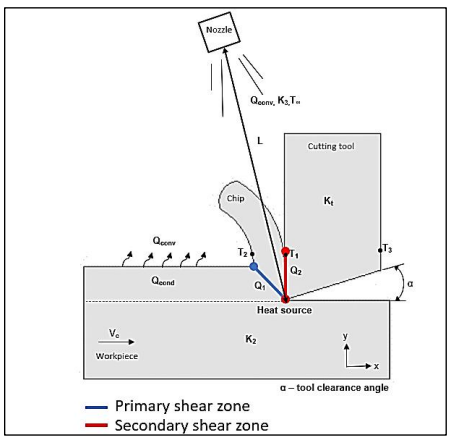

Figure 2: Cryo-CO_2 model

The heat generated during high-speed cutting was primarily transferred to cryo-CO_2, the workpiece, and the cutting tool through the primary and secondary shear zones, $Q_1 = K_w\nabla^2 T_w$ and $Q_2 = K_t\nabla^2 T_t$, respectively. Where, $\nabla^2 = \frac{\partial^2}{\partial x^2} + \frac{\partial^2}{\partial y^2} + \frac{\partial^2}{\partial z^2}$ was referred to Laplacian Operator in Cartesian coordinates. Thus, it can be simplified to:

$$(\Delta T)_f = \frac{[Q_1 + Q_2]\, L}{NuK_f} \tag{8}$$

Therefore, $(\Delta T)_f$ indicated that the temperature variances between the cryo-CO_2 and the surroundings drives the heat transfer. This temperature variance at the dispersed-continuous interface of cryo-CO_2 is governed by factors of $Q_1, Q_2, L, Nu,$ and K_f. Understanding the relationship between these input factors. The temperature variance is essential to optimize the cooling process for the cutting zone. Hence, the parameters for the simulation are shown in Table 1.

Table 1: Parameters for the simulation

Parameters	Values/conditions
Geometry	3-dimensional
Models	Single-phase, standard k-epsilon
Solver	Pressure-based, steady state
Solution method	SIMPLE pressure coupling scheme
Initialization	Hybrid
Nozzle diameter (mm)	1.3
Nozzle distance, L (mm)	20
Cryo-CO_2 flowrate (L/min)	15
Cryo-CO_2 pressure, P (Bar)	5
Cryo-CO_2 temperature, T (K)	206
Thermal conductivity of workpiece, K_w (W/mK)	11.338
Thermal conductivity of tool, K_t (W/mK)	87.812
Thermal conductivity of cryo-CO_2, K_f (W/mK)	0.0145

Mesh independence

A comprehensive mesh independence analysis was conducted to assess the impact of variations in the mesh parameters on both the accuracy and computational efficiency of CFD simulations performed using ANSYS Fluent. To handle complex geometries, a tetrahedral unstructured mesh was employed for solid geometry and fluid domain. The choice of using tetrahedral elements in the 3D complex geometry of the cutting zone model meshes are popular for modelling volumetric 3D geometry of objects due to their ability to effectively represent complex shapes and irregular geometries by Nakao et al. [22] and Yan et al. [23]. The 3D-symmetrical cryo-CO_2 model was simulated under two controlled factors: relevance centre (RC) and smoothing (S). The factors were controlled at three levels, with the temperature of cryo-CO_2 flow serving as the response variable, as shown in Table 2.

Table 2: Controlled factor and levels

Factors	Levels of factors		Response
	Actual	Coded	
Relevance centre	Coarse	-1	Cryo-CO_2 flow temperature
	Medium	0	
	Fine	1	
Smoothing	High	-1	
	Medium	0	
	Low	1	

In the Ansys approach, mesh refinement precision in the simulation outcomes was impacted by the RC. Three choices for the RC: coarse, medium, and fine specify different degrees of mesh refinement, as illustrated in Figure

3. Simultaneously, smoothing was a technique used to improve the mesh quality by adjusting the position of the mesh nodes. The low, medium, or high option controls the number of S iterations along with the threshold metric where the mesher will start smoothing [24]. Thus, these features collectively contribute to the accuracy and reliability of simulation outcomes.

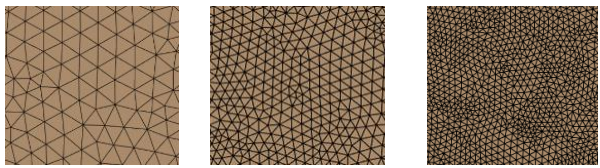

Figure 3: Relevance centre variations; (a) coarse, (b) medium, and (c) fine

Moreover, to minimize the number of simulations, time, and cost involved in arranging and optimizing mesh orders, the Design of Experiments (DOE) approach was utilized through Design Expert V13 software. Under this approach, 11 sets of mesh orders were developed using the RSM-CCD technique. This design method allows for exploring system response surfaces with respect to multiple variables by incorporating factorial points, axial points, and centre points. It enables the evaluation of both linear and quadratic effects of these variables [25]. In order to optimize and achieve a refined, smooth, and reliable cryogenic flow and maximize its cooling capacity, a statistical analysis approach was applied using a tool called Analysis of Variance (ANOVA). The ANOVA was also used to evaluate the impact of variation in control levels of mesh parameters on the response obtained through RSM-CCD. This allowed for comparing means and understanding variability within and between groups in the dataset.

Model validation - temperature

Validation involves comparing computational results with experimental data to assess their accuracy. The cryo-CO_2 flow from the nozzle was experimentally tested on the test bench to compare with the simulated results obtained from the CFD approach. The cryo-CO_2, which was supplied from a compressed cylinder of LCO_2 was injected through a nozzle with an inner diameter of 1.3 mm to the open air. The flow temperature was measured using a K-type thermometer [26]. The test bench setup, as shown in Figure 4, consisted of a board divided into quadratic sectors measuring 18 × 18 mm, along with a high-speed digital camera Olympus i-speed LT and five tungsten spotlights with power outputs set at 1000 W each to measure and record variations in cryo-CO_2 flow temperatures at different distances. In addition, all data acquisition parameters were established at a rate of 1500 frames per second.

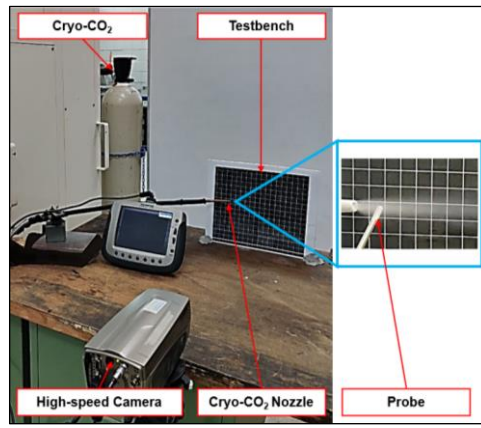

Figure 4: Test bench setup

Results and Discussion

Cryo-CO_2 flow temperature

The CCD and the corresponding temperature values from simulations were shown in the Table 3. The maximum temperature generated for the flow was 261 K in the coarse relevance centre, which led to less precise results. This is because coarse meshes have larger cell sizes, which can miss important details in the flow field. These discussions align seamlessly with Ferziger and Peric [27] research, where the larger cell sizes can also lead to numerical errors and inaccuracies in the simulation results. Meanwhile, 257 K was obtained from the medium and fine relevance center of mesh factors, thus showing that it was the lowest cryo-CO_2 flow temperature obtained, which was consistent with previous research by Pusavec et al. [28].

Statistical analysis using ANOVA

Based on the ANOVA results as shown in Table 4, the *F*-value of the model was 35.47 and the Prob>*F* was obviously smaller than 0.05. This implies that the model of RC is significant. Relevance center had a significant model term than alterations in the smoothing factor because it controls the resolution of the mesh, which is a fundamental aspect of the simulation [29]. This can result in a more accurate model that is more statistically significant.

For 3D complex geometry, the relevance center may be more effective than smoothing as it can better capture the statistical significance of the model terms. In general, the precision of the model can be supported by the coefficient of determination (adjusted R^2 and R^2) and residual plots. Since standard deviation = 0.75, R^2 = 89.86 %, and adjusted R^2 = 87.33 %, the model

fits statistically well. Even the predicted R^2 has a difference of less than 0.2 from the adjusted one, and adequate precision, which corresponds to signal-to-noise ratio, is much greater than 4, hence desirable [30]. Furthermore, the model is significant as a *p*-value if it is <0.05. The normal distribution data are guaranteed, and the maximum residual error is about 0.02. Suppose the *p*-value < 0.05 the parameters are considered significant. Overall, the statement suggests that the model is well-suited for the given data and can be used for further analysis and prediction.

Table 3: Simulation result for cryo-CO_2 flow temperature

Run no.	Factors		Response
	Relevance centre	Smoothing	Temperature
1	1	0	257
2	-1	-1	261
3	1	-1	257
4	0	1	258
5	0	0	257
6	-1	1	261
7	0	0	257
8	0	-1	258
9	0	0	257
10	1	1	258
11	-1	0	263

Table 4: ANOVA for quadratic fitting of cryo-CO_2 flow temperature

Source	Sum of squares	df	Mean square	*F*-values	*p*-value (Prob > *F*)	
Model	40.19	2	20.10	35.47	0.0001	Significant
A-Relevance Center	28.17	1	28.17	49.71	0.0001	
A^2	12.03	1	12.03	21.22	0.0017	
Residual	4.53	8	0.5667			
Lack of fit	4.53	6	0.7556			
R-squared	0.8986					
Adj. *R*-squared	0.8733					
Pred. *R*-squared	0.7904					
Adeq. precision	11.0229					

Development and validation of the second-order model using RSM

Equation (9) represented the establishment of the second order model equation for the flow temperature, based on the outcomes of the CFD simulation with the RSM-CCD software. The coded factors are as follows:

$$Temperature = 257.40 - 2.17A + 2.10A^2 \quad (9)$$

The model was then used to calculate the predicted cryo-CO_2 flow temperature. To validate and check the assumptions and adequacy of the statistical model, the diagnostic plots of the normal probability plot, and residuals vs. run as per Figures 5(a) and 5(b) were analysed. A normal probability plot of the residual can be plotted to confirm the check for normality assumption. In ANOVA, it usually more effective to do this with residuals. Thus, the normal probability plot graphs the residuals against the expected values were obtained from a normal distribution as depicted in Figure 4(a). All points lie close to the straight line, thus indicating that the data distribution closely approximates a normal distribution.

As per Figure 5(b), the residual versus run number plot exhibits a consistency and slight variance across each treatment that indicates that all the residual points are spread within upper and lower bounds, showing no patterns. This plot approves that the independence assumption is satisfied. Therefore, all the diagnostic plots indicate that all the required assumptions of ANOVA are met.

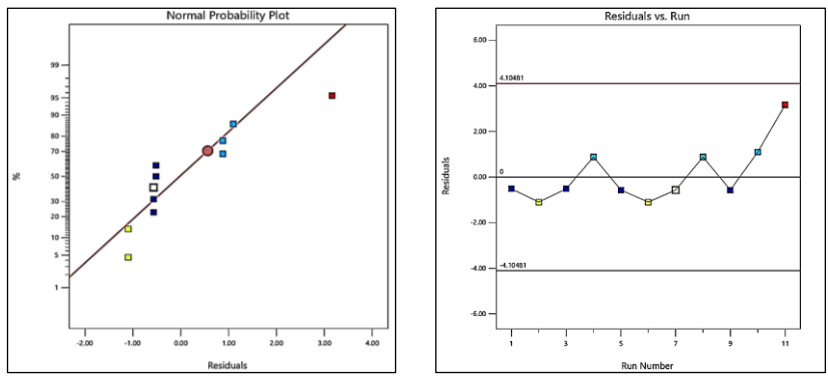

(a) (b)

Figure 5: Diagnostic plots for assumption of ANOVA; (a) normal probability plot of residuals, and (b) residuals vs run

Cryo-CO_2 flow temperature optimization

From model simulation using the numerical optimization method of the Design-Expert software, the optimum meshing factors conditions were suggested as follows: relevance centre at medium (0) and smoothing at medium (0). Suppose the model simulation was done under these conditions. In that case, the temperature, as predicted by the respective developed models, was 256.9 K, as indicated in Figure 6. This simulative predicted temperature generated from RSM-CCD was 8.47% different from experimental work.

However, a smaller prediction error which less than 10% indicated a better agreement between the model and the experimental data by Norma et al. [30]. Fact that when taking into account that real-world experiments may have inherent variability due to uncontrollable factors such as temperature fluctuations, unpredictable changes in the flowrate of cryo-CO_2. This variability may not be fully accounted for in the RSM-CCD model, leading to differences between predicted and experimental values. Despite that, this showed that the model is still adequate.

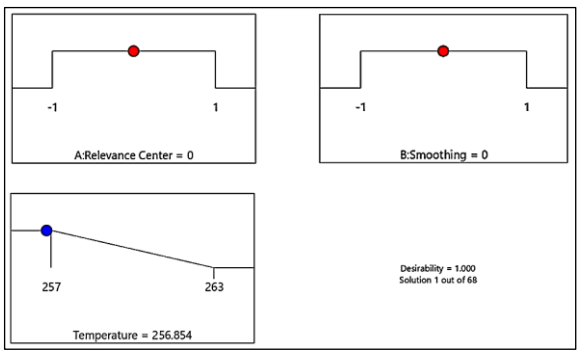

Figure 6: Ramp function graph of desirability as suggested by the RSM-CCD

Temperature vs nodes

To provide additional support for the optimal combination mesh controls obtained from the ANOVA analysis, a visual representation of the relationship between temperature and nodes was performed as per Figure 7. A gradual decrease in the cryo-CO_2 flow temperature was observed as the increased number of nodes as finer mesh of relevance centre, which can directly impact the accuracy of the simulation results. The trendline analysis revealed that a constant trendline was achieved at 197135 nodes where at medium for both mesh-controlled factors. Nevertheless, further increased the number of nodes would not significantly impact on trend of the simulation results because it would lead to increased computational workload and analysis time. Furthermore, too many fine grids may sharply increase the round-off error beyond the truncation error. Conversely, coarse meshes create a significant spatial discretization error, reducing the analysis results' accuracy [31]. This is contrary to the research found by D'Addona et al. [35], where finer mesh was chosen in the development of 3D geometry. This is due to the fact that the researcher just modelled the cutting tool only so that only required even though fine mesh also requires more computational time and resources, there is a trade-off between accuracy and efficiency, unlike this current study, where consist of more than one bodies. Additionally, the ANOVA optimization is validated by the close match between the simulated mesh and ANOVA result,

demonstrating a 13.56% percentage error in the absolute error analysis. Taking into account the uncertainties in the simulation process, the error level demonstrated a reasonable agreement between the ANOVA results and the CFD simulation. Regarding to Revie et al. [32], an acceptable result was considered a percentage error of less than 20%, with errors ranging from ± 10 – 20 % being common. Thus, this particular number of nodes at medium RC – medium S was selected for further analysis as it was sufficient to achieve the desired efficiency of cryo-CO_2 flow in CFD simulations, which consistent with Xu et al. [33] studies.

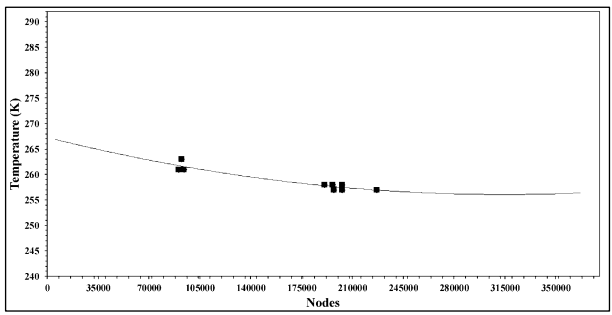

Figure 7: Temperature vs nodes: achieving mesh independence

Model validation

The results obtained from the DOE yielded one optimal solution where medium was in RC and S, respectively, in the simulation. Figure 8 presents the simulated cryo-CO_2 data using proposed models and experimental data. From 3.6 to 18 mm of length flow, both bar graphs showed trends steadily rose from its lowest cryo-CO_2 flow temperature until reached at their highest cryogenic flow temperature. This is because the flow was exposed and absorbed heat from its surroundings, including the ambient air and heat generated at the cutting area. This heat absorption can further contributed to a increased in temperature as the cryo-CO_2 flow moves towards the cutting zone as regarding to the studies by Ross et al. [34], where the machining process generated a lot of heat due to friction and deformation. In addition, Gutzeit et al. [35] also performed cryo-CO_2 outlet at -78.5 °C. However, the author did not specify the exact temperature of the cryogenic coolant at the cutting zone but was likely to be higher than the outlet temperature due to heat transfer from the workpiece and tool. Nevertheless, Arunprasath et al. [36] found that the cryogenic media still can help to lower the temperature of the cutting zone and improve the machining performance and quality.

On the other hand, the error bars (maximum ± 5) represent the standard deviation of triplicate experimental runs at the corresponding cryo-CO_2 temperature flow. The comparison revealed the percentage of standard

deviation on simulation and experimental work lies within ~ 0.4 – 0.6 % and ~ 0.4 – 4.2 % of the observed values of cryo-CO_2 temperature. Furthermore, in many fields a deviation of less than 10% between simulation and experimental results is often considerable acceptable [30]. Overall, the experimental temperature has larger error bars at 7.2 mm, which may be due to factors such as heat losses, radiation, or other thermal effects may become more pronounced, introducing uncertainties in the experimental measurements.

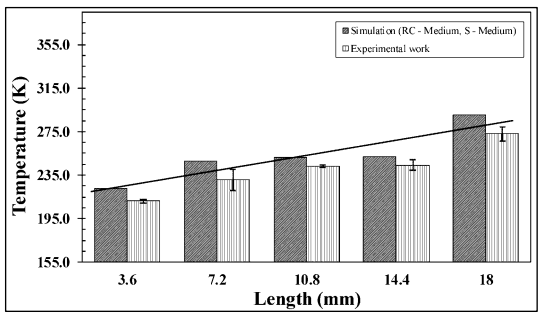

Figure 8: Comparison between simulated and experimented cryo-CO_2 temperature

Performance of cryo-CO_2 temperature on CFD

Additional research was conducted to examine the effects of the cutting zone in the machining process and evaluated how the cryo-CO_2 performed to improve the machining performance and quality. Further analysis was carried out to analyse the heat generation at the cutting zone using the optimal data selected from the model validation. The visual depicted in Figure 9 showed where heat was generated during the metal cutting resulted heat conduction at Q_1 (points A to B) and Q_2 (points B to C), respectively.

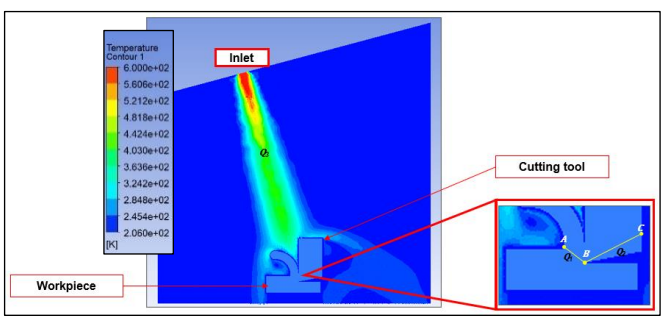

Figure 9: CFD simulation results for medium (RC) and medium (S)

The primary shear deformation was occurred at Q_1, where intense plastic deformation occurred at chip-tool, leading to significant heat generation due to the conversion of mechanical work into heat [37]. From point A to B as shown in Figure 10(a), the heat conduction was linearly decreased to the point B. However, the increase in heat conduction at the secondary shear zone, as indicated by the polynomial trendline as per Figure 10(b), where located between the metal chip and the cutting tool was noticeably higher than Q_1. Contrary to Ogedengbe et al. [38], where particularly the primary deformation zone (shear zone) consuming about 70% of the total energy applied. However, in the present study, Q_2 was higher heat than Q_1 due to the energy supplied was converted into heat energy had faced the intense rubbing and friction at the chip-tool interface during high-speed machining. In addition, choice of using a tungsten carbide cutting tool in the simulation as this material known for their hardness and wear resistance thus can generate quality [39].

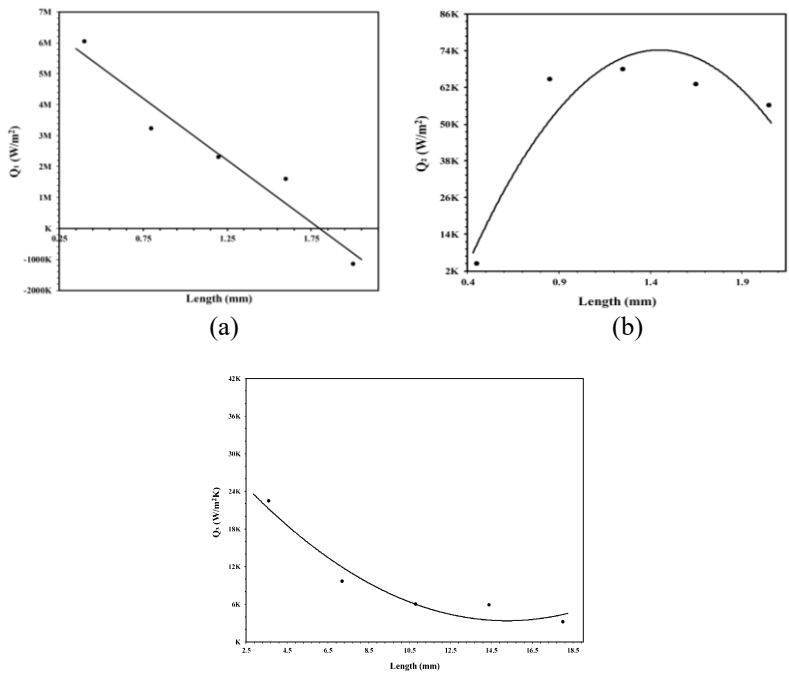

Figure 10: Heat transfer mechanism; (a) heat conduction at Q_1, (b) heat conduction at Q_2, and (c) heat convection at Q_3

Thus, cryo-CO_2 was utilised as it likely absorbs heat from the cutting zone and carries it away through convection as per Figure 10(c), contributing

to effective heat dissipation. Heat convection (Q_3) transferred of heat through the movement of a fluid (in this case, cryo-CO_2 undergoes a phase change, transitioning from a liquid to a gaseous state) carrying heat away from the hot surfaces. The gaseous cryogenic carbon dioxide, enriched with absorbed heat, convects away from the cutting zone [40]. This convective flow creates a cooling effect by carrying the absorbed heat to areas where it can be dissipated more effectively. Overall confirmed that the cryo-CO_2 flow was reached the tool tip as point B produced considerably lower temperature than point C.

Temperature variation

To gain a comprehensive understanding of the temperature variation within the cryo-CO_2 flow, two essential graphs have been employed through the flow distance: the Nusselt number and heat transfer coefficient. These graphical representations as shown in Figure 11 provide a visual depiction of both affected the cutting zone.

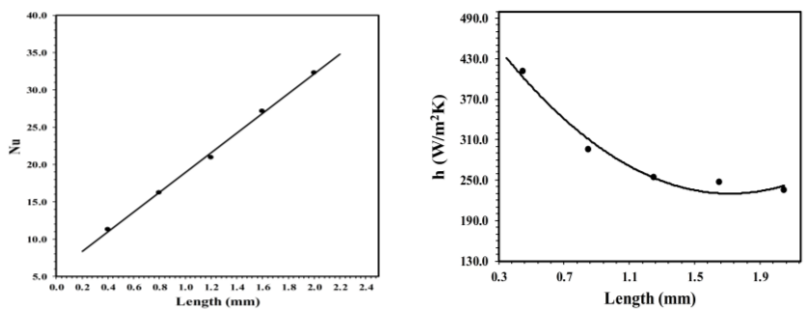

(a) (b)

Figure 11: Temperature variations across the length at Q_3; (a) Nusselt number, and (b) heat transfer coefficient

As per Figure 11(a), it was observed that the Nusselt number was directly proportional to the flow distance, which strongly suggests that the ratio of convective heat transfer is much larger than the ratio of conductive heat transfer in the system, as revealed by the definition of Nusselt number itself [41]. As the flow distance increased, the convective heat transfer became more dominant, while the conductive heat transfer became less significant. This is because the cryo-CO_2 dispersed had more time to exchange heat with their surroundings, leading to a more efficient heat transfer process. This suggests that the cryo-CO_2 flow can effectively remove more heat from the contact surface at the workpiece. Contrast to the trendline of the heat transfer coefficient graph gradually decreased as the flow distance increased as it undergoes a phase change from liquid to gas due to the high latent heat of sublimation. Wang et al. [42] stated that, this phase change reduces the density

and the specific heat capacity of the cryo-CO_2 flow, which in turn reduces the convective heat transfer coefficient as shown in Figure 11(b).

Conclusion

In this study, a simulation technique by ANSYS Fluent was used to perform a mesh analysis for mesh independence test to identify the optimal mesh parameters for CFD of cryo-CO_2 model. The mesh factors of the tetrahedral unstructured grid were designed (relevance center and smoothing) using CCD and optimized their response on the cryo-CO_2 flow temperature using ANOVA. The optimal mesh combination was obtained at medium coded level for both relevance center and smoothing meshes which at the lowest cryo-CO_2 flow temperature of 256.85 K. Validation through experimental work revealed the percentage of standard deviation on simulation and experimental work lies within ~0.4 – 0.6% and ~0.4 – 4.2% of the observed values of cryo-CO_2 temperature for flow distances between 3.6 to 18 mm. Additional research was also conducted to enhance further the understanding of fluid dynamics and heat transfer characteristics in metal cutting using cryogenic CO_2 cooling. Consequently, this study demonstrated that cryogenic cooling in machining has advantages such as decreased cutting temperatures, ultimately resulting in more efficient and productive machining procedures.

Contributions of Authors

The authors confirm the equal contribution in each part of this work. All authors reviewed and approved the final version of this work.

Funding

This work was supported by the Ministry of Higher Education (MOHE) Malaysia and Universiti Teknologi MARA, under the Fundamental Research Grant Scheme: Grant No. FRGS/1/2022/TK08/UITM/02/48 and 600-RMC/FRGS 5/3 (048/2022).

Conflict of Interests

One of the authors, Nurul Hayati Abdul Halim, is a section editor of the Journal of Mechanical Engineering (JMechE). The other authors have no other conflict of interest to note.

Acknowledgment

We would like to express our gratitude to the College of Engineering and Research Management Centre (RMC), Universiti Teknologi MARA for providing the necessary equipment that enabled us to conduct this research effectively.

References

[1] O. Pereira, A. Celaya, G. Urbikaín, A. Rodríguez, A. Fernández-Valdivielso, and L. Noberto López de Lacalle, "CO2 cryogenic milling of Inconel 718: Cutting forces and tool wear," *Journal of Materials Research and Technology*, vol. 9, no. 4, pp. 8459–8468, 2020, doi: 10.1016/j.jmrt.2020.05.118.

[2] D. Grguraš, L. Sterle, P. Krajnik, and F. Pušavec, "A novel cryogenic machining concept based on a lubricated liquid carbon dioxide," *International Journal of Machine Tools and Manufacture*, vol. 145, p.103456, 2019, doi: 10.1016/j.ijmachtools.2019.103456.

[3] C. MacHai and D. Biermann, "Machining of β-titanium-alloy Ti-10V-2Fe-3Al under cryogenic conditions: Cooling with carbon dioxide snow," *Journal of Materials Research and Technology*, vol. 211, no. 6, pp. 1175–1183, 2011, doi: 10.1016/j.jmatprotec.2011.01.022.

[4] N. H. A. Halim, C. H. C. Haron, J. A. Ghani, and M. F. Azhar, "Tool wear and chip morphology in high-speed milling of hardened Inconel 718 under dry and cryogenic CO2 conditions," *Wear*, vol. 426–427, no.B, pp. 1683–1690, 2019, doi: 10.1016/j.wear.2019.01.095.

[5] O. Pereira, A. Rodríguez, J. Barreiro, A. I. Fernández-Abia, and L. N. L. de Lacalle, "Nozzle design for combined use of MQL and cryogenic gas in machining," *International Journal of Precision Engineering and Manufacturing-Green Technology*, vol. 4, no. 1, pp. 87–95, 2017, doi: 10.1007/s40684-017-0012-3.

[6] B. Dilip Jerold and M. Pradeep Kumar, "Experimental investigation of turning AISI 1045 steel using cryogenic carbon dioxide as the cutting fluid," *Journal of Manufacturing Processes*, vol. 13, no. 2, pp. 113–119, 2011, doi: 10.1016/j.jmapro.2011.02.001.

[7] E. Tahmasebi, P. Albertelli, T. Lucchini, M. Monno, and V. Mussi, "CFD and experimental analysis of the coolant flow in cryogenic milling," *International Journal of Machine Tools and Manufacture*, vol. 140, pp. 20–33, May 2019, doi: 10.1016/j.ijmachtools.2019.02.003.

[8] M. Jamil *et al.*, "Heat Transfer Efficiency of Cryogenic-LN2 and CO2-snow and their application in the Turning of Ti-6AL-4V," *International Journal of Heat and Mass Transfer*, vol. 166, p. 120716, 2021, doi: 10.1016/j.ijheatmasstransfer.2020.120716.

[9] A. Kumar, R. Bhardwaj, and S. S. Joshi, "Thermal analysis of drilling in titanium under flood and cryogenic cooling using coupled CFD and FEM," *Journal of Manufacturing Processes*, vol. 81, pp. 605–623, 2022, doi: 10.1016/j.jmapro.2022.06.075.

[10] K. Gamidi, V. K. Pasam, and P. A. K. Lam, "A numerical investigation on coolant flow and heat transfer characteristics of cutting tool in spot cooled vibration assisted turning of Ti6Al4V alloy," *International Journal of Thermal Sciences*, vol. 191, p. 108394, 2023, doi: 10.1016/j.ijthermalsci.2023.108394.

[11] Z. Wu, S. Li, G. Yuan, D. Lei, and Z. Wang, "Three-dimensional numerical study of heat transfer characteristics of parabolic trough receiver," *Applied Energy*, vol. 113, pp. 902–911, 2014, doi: 10.1016/j.apenergy.2013.07.050.

[12] R. Mohan, S. Shrikhande, V. Joshi, and R. Harish, "Numerical Investigation on Thermal Performance of Duplex Nanocoolant Jets in Drilling of Ti-6Al-4V Alloy," *Applied Sciences*, vol. 12, no. 22, pp. 1-17, 2022, doi: 10.3390/app122211715.

[13] I. Sadrehaghighi, "Mesh Sensitivity & Independence Study," *CFD Open Series*, no. May, pp. 1–50, 2020, doi: 10.13140/RG.2.2.34847.51365/2.

[14] J. R. Hendry, J. G. M. Lee, and M. J. Battrum, "CFD model of fluid flow and particle deposition during cryogenic condensation," *Chemical Engineering Research and Design*, vol. 143, pp. 201–214, 2019, doi: 10.1016/j.cherd.2019.01.016.

[15] S. H. Kim, S. W. Lee, S. Han, and S. M. Kim, "Numerical investigation of thermal characteristics of spray cooling with minimum quantity lubrication in milling process," *Applied Mathematical Modelling*, vol. 65, pp. 137–147, 2019, doi: 10.1016/j.apm.2018.08.011.

[16] J. Caudill, J. Schoop, and I. S. Jawahir, "Numerical Modeling of Cutting Forces and Temperature Distribution in High Speed Cryogenic and Flood-cooled Milling of Ti-6Al-4V," *Procedia CIRP*, vol. 82, pp. 83–88, 2019, doi: 10.1016/j.procir.2019.04.055.

[17] M. Hamzaabdulsada, "Finite Element Analysis of Fins with Convection and Radiation Heat Transfer," *Al-Qadisiyah Journal For Engineering Sciences*, vol. 8, no. 2, pp. 242–258, 2015

[18] A. Singh, V. Dubey, and A. Kumar Sharma, "Thermal modelling of cutting tool under different cutting environment in turning," *Materials Today Proceedings*, 2023, doi: 10.1016/j.matpr.2023.04.193.

[19] P. Lequien, G. Poulachon, J. C. Outeiro, and J. Rech, "Hybrid experimental/modelling methodology for identifying the convective heat transfer coefficient in cryogenic assisted machining," *Applied Thermal Engineering*, vol. 128, pp. 500–507, 2018.

[20] R. Misra *et al.*, "Prediction of behavior of triangular solar air heater duct using V-down rib with multiple gaps and turbulence promoters as artificial roughness: A CFD analysis," *International Journal of Heat and*

Mass Transfer, vol. 162, pp. 1-19, 2020, doi: 10.1016/j.ijheatmasstransfer.2020.120376.

[21] S. A. Khan, O. M. Ibrahim, and A. Aabid, "CFD analysis of compressible flows in a convergent-divergent nozzle," *Materials Today Proceedings*, vol. 46, part.7, pp. 2835–2842, 2021, doi: 10.1016/j.matpr.2021.03.074.

[22] M. Nakao, "Vertex-preserving Cutting of Elastic Objects," *IEEE,* pp. 277–278, 2008, doi: 10.1109/VR.2008.4480799

[23] C. Yan, "A three - dimensional heat transfer and thermal cracking model considering the effect of cracks on heat transfer," *International Journal for Numerical and Analytical Methods in Geomechanic*, vol. 43, no. 10, pp. 1825–1853, 2019, doi: 10.1002/nag.2937.

[24] Z. Zulkifli, N. H. A. Halim, Z. H. Solihin, J. Saedon, A. A. Ahmad, A. H. Abdullah, N. A. Raof and M. A. Hadi, "The analysis of grid independence study in continuous disperse of MQL delivery system," *Journal of Mechanical Engineering and Sciences,* vol. 17, no. 3, pp. 9586–9596, 2023, doi: 10.15282/jmes.17.3.2023.5.0759

[25] A. A. Ahmadi, M. Arabbeiki, H. M. Ali, M. Goodarzi, and M. R. Safaei, "Configuration and optimization of a minichannel using water–alumina nanofluid by non-dominated sorting genetic algorithm and response surface method," *Nanomaterials*, vol. 10, no. 5, pp. 1-20, 2020, doi: 10.3390/nano10050901.

[26] Y. Abdelaziz, M. Hammam, F. Megahed, and E. R. Qamar, "Characterizing Drift Behavior in Type K and N Thermocouples After High Temperature Thermal Exposures," *Journal of Advanced Research in Fluid Mechanics and Thermal Sciences*, vol. 97, no. 1, pp. 62–74, 2022, doi: 10.37934/arfmts.97.1.6274

[27] J. H. Ferziger and I. M. Peric, Computational Methods for Fluid Dynamics, 3rd Edition, Springer International Publishing, Germany, 2019.

[28] F. Pušavec, D. Grguraš, M. Koch, and P. Krajnik, "Cooling capability of liquid nitrogen and carbon dioxide in cryogenic milling," *CIRP Annals*, vol. 68, no. 1, pp. 73–76, 2019, doi: 10.1016/j.cirp.2019.03.016.

[29] T. M. I. T. Faculty, A. Published, S. Us, and P. Url, "Moving mesh adaptation for Si and Moving Mesh Adaptation for Si and GaN Based Power Device Simulation", *Journal of Computational Electronics,* vol. 17, pp. 1621–1629, 2018,doi: 10.1007/s10825-018-1218-5

[30] D. M. Norma F. Hubele, George C. Runge, *Engineering Statistics, 5th Edition*, 5th Editio. 2010.

[31] C. Liu, J. Tu, and G. H. Yeoh, Computational Fluid Dynamics: A Practical Approach, 3rd Edition, Elsevier Science, Netherlands, 2018.

[32] J. A. Revie *et al.*, "Evaluation of a model-based hemodynamic monitoring method in a porcine study of septic shock," *Computational and mathematical methods in medicine*, vol. 2013, pp. 1-17, 2013, doi: 10.1155/2013/505417.

[33] X. Xu, H. Li, and Y. Lin, "Mesh-Order Independence in CFD Simulation," *IEEE Access*, vol. 7, pp. 119069–119081, 2019, doi: 10.1109/ACCESS.2019.2937450.

[34] K. N. S. Ross and G. Manimaran, "Machining Investigation of Nimonic-80A Superalloy Under Cryogenic CO2 as Coolant Using PVD-TiAlN/TiN Coated Tool at 45° Nozzle Angle," *Arabian Journal for Science and Engineering*, vol. 45, no. 11, pp. 9267–9281, Nov. 2020, doi: 10.1007/s13369-020-04728-8.

[35] K. Gutzeit, G. Bulun, G. Stelzer, B. Kirsch, J. Seewig, and J. C. Aurich, "Sub - zero milling of Ti - 6Al - 4V — impact of the cutting parameters on the resulting forces , tool wear , and surface quality," *The International Journal of Advanced Manufacturing Technology*, vol. 126, pp. 3367–3381, 2023, doi: 10.1007/s00170-023-11334-z.

[36] K. Arunprasath, A. Thivagar, P. Mathan, and P. Yuvanarasimman, "Cryogenic turning of titanium alloys: Machinability characteristics and environmental consequences," *Materials Todays Proceedings*, vol. 66, pp. 749–753, 2022, doi: 10.1016/j.matpr.2022.04.047.

[37] N. A. Abukhshim, P. T. Mativenga, and M. A. Sheikh, "Heat generation and temperature prediction in metal cutting: A review and implications for high speed machining," *International Journal of Machine Tools and Manufacture*, vol. 46, no. 7–8, pp. 782–800, 2006, doi: 10.1016/j.ijmachtools.2005.07.024.

[38] T. S. Ogedengbe *et al.*, "The Effects of Heat Generation on Cutting Tool and Machined Workpiece," *Journal of Physics: Conference Series*, vol. 1378, no. 2, pp. 1-10, 2019, doi: 10.1088/1742-6596/1378/2/022012.

[39] H. Lu, C. Zhao, H. Wang, X. Liu, R. Yu, and X. Song, "Hardening tungsten carbide by alloying elements with high work function," *Acta Crystallographica Section B Structural Science, Crystal Engineering and Materials*, vol. 75, no. 6, pp. 994–1002, 2019.

[40] S. Chaabani, I. Rodriguez, M. Cuesta, Y. Ayed, P. J. Arrazola, and G. Germain, "Tool wear and cutting forces when machining inconel 718 under cryogenic conditions: Liquid nitrogen and carbon dioxide," *AIP Conference Proceedings*, pp. 1-6, 2019, doi: 10.1063/1.5112610.

[41] K. Kumar, C. El Mohtar, and R. Gilbert, "Conductive and Convective Heat Transfer in Inductive Heating of Subsea Buried Pipelines," *Journal of Pipeline Systems Engineering and Practice*, vol. 13, no. 4, pp. 1–31, 2022, doi: 10.1061/(asce)ps.1949-1204.0000672.

[42] Y. Wang, M. Dai, K. Liu, J. Liu, L. Han, and H. Liu, "Research on surface heat transfer mechanism of liquid nitrogen jet cooling in cryogenic machining," *Applied Thermal Engineering.*, vol. 179, p. 115607, 2020, doi: 10.1016/j.applthermaleng.2020.115607.